Contribution of the Hydrophobic Effect to the Stability of Human Lysozyme: Calorimetric Studies and X-ray Structural Analyses of the Nine Valine to Alanine Mutants[†,‡]

Kazufumi Takano,[§] Yuriko Yamagata,[||] Satoshi Fujii,[||] and Katsuhide Yutani*[,§]

Institute for Protein Research and Faculty of Pharmaceutical Sciences, Osaka University, Yamadaoka, Suita, Osaka 565, Japan

Received August 27, 1996[⊗]

ABSTRACT: To clarify the contribution of the hydrophobic effect to the conformational stability of human lysozyme, a series of Val to Ala mutants were constructed. The thermodynamic parameters for the denaturation of these nine mutant proteins were determined using differential scanning calorimetry (DSC), and the crystal structures were solved at high resolution. The denaturation Gibbs energy ($\Delta\Delta G$) and enthalpy ($\Delta\Delta H$) values of the mutant proteins ranged from +2.2 to −6.3 kJ/mol and from +7 to −17 kJ/mol, respectively. The structural analyses showed that the mutation site and/or the residues around it in some proteins shifted toward the created cavity, and the substitutions affected not only the mutations site but also other parts far from the site, although the structural changes were not as great. Correlation between the changes in the thermodynamic parameters and the structural features of mutant proteins was examined, including the five Ile to Val mutant human lysozymes [Takano et al. (1995) *J. Mol. Biol. 254*, 62−76]. There was no simple general correlation between $\Delta\Delta G$ and the changes in hydrophobic surface area exposed upon denaturation ($\Delta\Delta ASA_{HP}$). We found only a new correlation between the $\Delta\Delta G$ and $\Delta\Delta ASA_{HP}$ of all of the hydrophobic residues if the effect of the secondary structure propensity was taken into account.

Hydrophobic interactions are the major factor stabilizing the folded conformations of proteins (Kazumann, 1959). Studies of hydrophobic mutants of proteins [e.g., Yutani et al. (1977, 1987), Matsumura et al. (1988), Kellis et al. (1988, 1989), Shortle et al. (1990), Eriksson et al. (1992), and Jackson et al. (1993)] have shown that the hydrophobic residues in a protein contribute to the stability but the contribution differs with the location. For example, nine different Ile to Val substitutions are associated with denaturation Gibbs energy changes that range from 2.1 to 7.5 kJ/mol (Matthews, 1993). To understand these differences, several ideas have been proposed (Serrano et al., 1992; Pace, 1992; Eriksson et al., 1992) but they do not reconcile all of the observations. Therefore, in order to understand the role of hydrophobic residues in protein stability, more detailed information from mutant proteins should be systematically and comprehensively accumulated on the thermodynamic parameters of the denaturation using differential scanning calorimetry and on the structures at high resolution by X-ray crystallography.

Calorimetry and X-ray structural analyses have been used to study human lysozymes of Pro mutants (Herning et al., 1992), disulfide mutants (Kuroki et al., 1992a), and a calcium-binding mutant (Kuroki et al., 1992b). We have also reported studies of hydrophobic mutant human lysozymes in which Ile was substituted by Val in the interior of the molecule resulting in the deletion of a methylene group (Takano et al., 1995). To elucidate the role of hydrophobic residues of human lysozyme in conformational stability, we focused on the Val residues located in various regions in the protein. Each residue was substituted by Ala which removes two methylene group equivalents. Human lysozyme (130 residues, 4 S−S bridges) contains nine Val residues, as shown in Figure 1. The side-chains of Val93, Val99, and Val100 are in an α-helix and are nearly completely buried in the protein. The side-chains of Val121, Val125, and Val130 in the C-terminal region are also mostly buried in the inside of the molecule. In contrast, the side-chains of Val2, Val74, and Val110 are mostly exposed to solvent in the native protein (Table 1).

In this paper, the thermodynamic parameters characterizing the denaturation of the nine Val mutants were determined using scanning calorimetry, and their three-dimensional structures were determined at high resolution by X-ray crystallography. We will use these results to gain a better understanding of the hydrophobic effect.

EXPERIMENTAL PROCEDURES

Mutant Proteins. Mutagenesis, expression and purification of the Val mutant human lysozymes were performed as described (Takano et al., 1995). Furthermore, the prepara-

[†] This work was supported in part by Fellowships from the Japan Society for the Promotion of Science for Japanese Junior Scientists (K.T.) and by a grant-in-aid for special project research from the Ministry of Education, Science, and Culture of Japan (K.Y.).

[‡] Coordinates have been deposited in the Brookhaven Protein Data Bank under PDB File Names V100A, 1OUB; V110A, 1OUC; V121A, 1OUD; V125A, 1OUE; V130A, 1OUF; V2A, 1OUG; V74A, 1OUH; V93A, 1OUI; and V99A, 1OUJ.

* Corresponding author. Tel: +81-6-879-8615. FAX: +81-6-879-8616. E-mail: yutani@protein.osaka−u.ac.jp.

[§] Institute for Protein Research.

[||] Faculty of Pharmaceutical Sciences.

[⊗] Abstract published in *Advance ACS Abstracts,* January 1, 1997.

[1] Abbreviations: ASA, accessible surface area; $\Delta\Delta ASA_{HP}$, changes in hydrophobic surface area exposed upon denaturation; ΔC_p, heat capacity change; ΔG, Gibbs energy change; ΔH, enthalpy change; DSC, differential scanning calorimetry; rms, root mean square; T_d, denaturation temperature.

S0006-2960(96)02182-4 CCC: $14.00

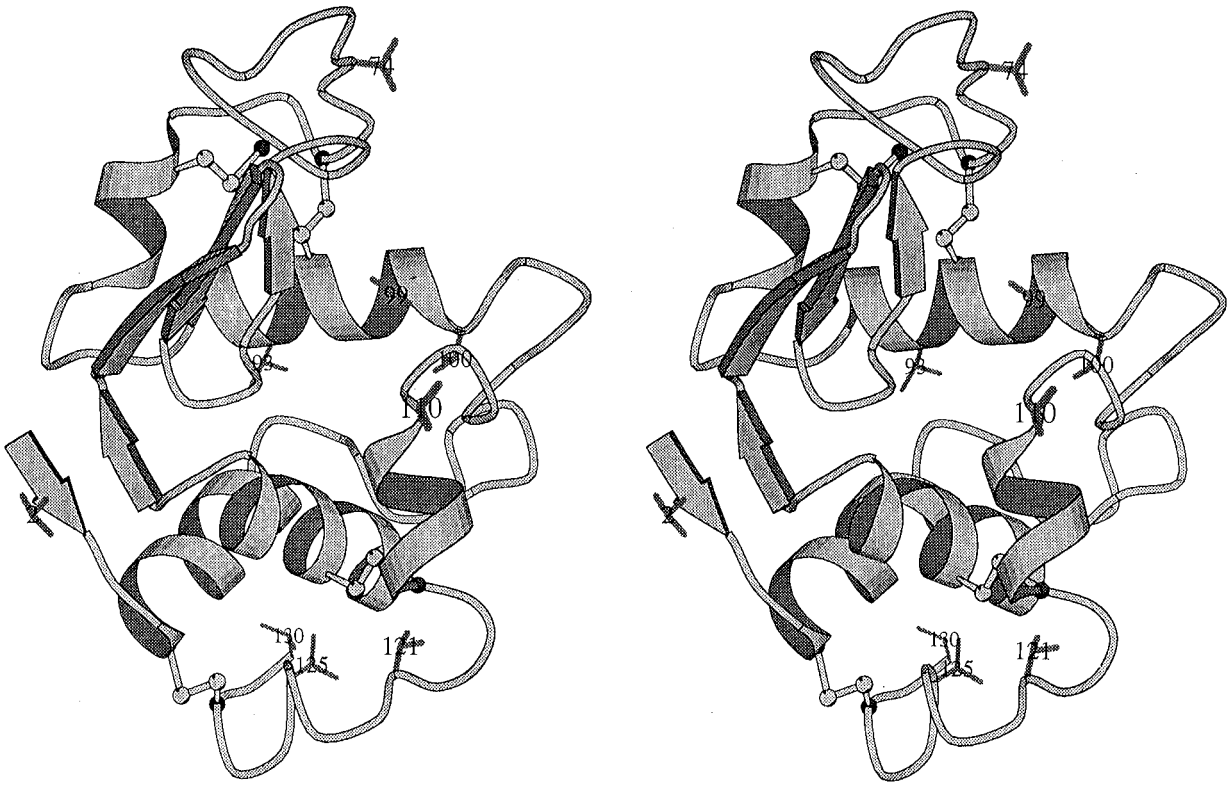

FIGURE 1: Stereodrawing of the wild-type human lysozyme structure. The positions of the substituted Val residues are indicated. The structure was generated by the program MOLSCRIPT (Kraulis, 1991). The circles with dots represent sulfur atoms of disulfide bonds.

Table 1: Structural Characteristics of Val Residues in the Wild-Type Human Lysozyme[a]

	ASA (%)[b]	χ_1 (deg)
Val2	72	−178
Val74	75	−84
Val93	3.0	174
Val99	1.9	175
Val100	0	−57
Val110	71	174
Val121	15	−69
Val125	16	−66
Val130	2.4	−65

[a] Takano et al. (1995). [b] ASA (%) = [ASA(Val)^{fold}/ASA(Val)^{extended}] × 100. The ASA(Val)^{extended} is the value for a polypeptide as a reference for the unfolded state (Oobatake & Ooi, 1993). The ASA was calculated using the procedure of Connolly (1985, 1993) with a probe radius of 1.4 Å.

tions for V74A, V100A, and V110A were applied to an Asahipak ES-502C column and were eluted with a linear gradient of 0−0.36 M Na_2SO_4 in 0.05 M sodium phosphate buffer at different pH (pH 5.5) because the heat denaturation curves of these mutant proteins gave two peaks in calorimetric measurements. The proteins collected from the main peak showed a single transition curve in DSC. The mass spectrum (Sciex API.III mass spectrometer) of the purified proteins was used to confirm the identify of the mutant proteins. All chemicals were reagent grade. Protein concentration was determined spectrophotometrically using $E^{1\%}_{1cm} = 25.65$ at 280 nm (Parry et al., 1969).

Differential Scanning Calorimetry (DSC). Calorimetric measurements and data analyses were carried out as described (Takano et al., 1995). In brief, a DASM4 adiabatic microcalorimeter equipped with an NEC personal computer was used. The scan rate was 1.0 K/min. The sample solutions were prepared by dissolution in 0.05 M glycine buffer between pH 2.5 and 3.2, and the sample concentrations were 0.7−1.5 mg/mL. Data analysis was done using the Origin software (MicroCal Inc., Northampton, MA).

X-ray Crystallography. Mutant human lysozymes were crystallized, diffraction data collected, and the structures refined as described (Takano et al., 1995). In short, the crystals (>0.2 × 0.2 × 0.3 mm^3) grew in 2.5 M NaCl−0.02 M acetate (pH 4.5) at 10 °C. All the crystals belong to the space group $P2_12_12_1$. The diffraction data were collected at 10 °C by the oscillation method on a Rigaku R-AXIS IIC imaging plate mounted on a Rigaku RU300 rotating anode X-ray generator (Cu Kα radiation, 40 kV, 200 mA). All refinements were performed by the program X-PLOR (Brunger, 1992) using the coordinates of the wild-type structure (Takano et al., 1995). Solvent molecules were detected using the program FLAPPER (S. Fujii, unpublished). The numerical calculations, in part, were carried out on NEC engineering workstations at the Research Center for Protein Engineering, Institute for Protein Research, Osaka University.

RESULTS

Differential Scanning Calorimetry (DSC) of Mutant Human Lysozymes. In order to determine the thermodynamic parameters of denaturation, DSC measurements of Val to Ala mutant human lysozymes were made at acidic pHs between 2.5 and 3.2. In this pH region, the denaturation of the mutants was reversible. Typical excess heat capacity curves are shown in Figure 2. The examined proteins gave similar results. The denaturation temperature (T_d), the calorimetric enthalpies (ΔH_{cal}), the van't Hoff enthalpies (ΔH_{vH}), and the heat capacity changes (ΔC_p) were obtained directly from analyses of these curves (Table 2). The T_d values were sensitive to pH and increased linearly with pH.

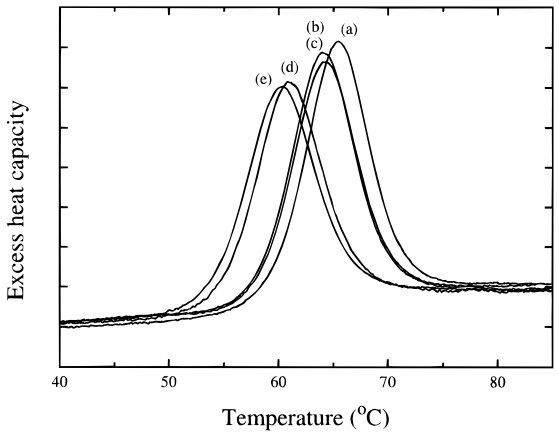

FIGURE 2: Typical excess heat capacity curves of the wild-type and mutant human lysozymes at pH 2.71. (a) Wild-type; (b) V74A; (c) V100A; (d) V125A; and (e) V2A. The increments of excess heat capacity were 10 kJ/mol K.

The temperature dependences of ΔH_{cal} for the nine Val mutant lysozymes were linear. The ΔC_p values were obtained from the slopes by least-squares fitting (Table 3). These ΔC_p values were coincident within experimental error with the average of the values obtained from the excess heat capacity curves (Table 2).

The thermodynamic parameters for denaturation of the mutant proteins at the denaturation temperature of the wild-type protein, 64.9 °C, and at pH 2.7 were calculated (Table 3) using the following equations:

$$\Delta H(T) = \Delta H(T_d) - \Delta C_p(T_d - T) \quad (1)$$

$$\Delta S(T) = \Delta H(T_d)/T_d - \Delta C_p \ln(T_d/T) \quad (2)$$

$$\Delta G(T) = \Delta H(T) - T\Delta S(T) \quad (3)$$

and assuring that ΔC_p does not depend on temperature (Privalov & Khechinashvili, 1974).

As shown in Table 3, the effects of the deletion of two methylene groups (Val → Ala) on the stability of human lysozyme were different in each mutant protein. The changes in ΔG ranged from +2.2 to −6.3 kJ/mol, and the changes in ΔH ranged from +7 to −17 kJ/mol, compared with the wild-type protein.

X-ray Structures of Mutant Human Lysozymes. Data collection and refinement statistics for the nine Val to Ala mutant human lysozymes are summarized in Table 4. The mutant structures seemed to be essentially the same fold as the wild-type structure except at the substituted residue. The rms deviations and the changes in the *B*-factors of each residue for the main-chain atoms between the wild-type and each mutant are shown in Figures 3a−i and 4a−i, respectively. Figures 3j and 4j show those between V74A and V74A2, respectively. V74A2 is the structure of the same protein obtained from smaller crystal to estimate the errors in our structures. In Figure 3, there were no differences more than 0.4 Å between the mutant and wild-type structures except for the C-terminal regions of V125A and V130A. The differences between V74A and V74A2 are small: the averages of the rms deviations for all of the atoms and the main-chain atoms were 0.11 and 0.06 Å, respectively. Judging from this reference (Figure 3j), differences over 0.2 Å might reflect meaningful structural change, and indicate that substitutions affect the area around the mutation site and also other parts of the molecule far from the site. For most of the mutant proteins, the largest shift was near residues 71−74, a loop on the surface with the largest *B*-factors in the protein. In Figure 4, the *B*-factors of some mutants are larger than those of the wild-type, especially V2A. This might be due to the smaller crystal size of the V2A mutant. Note that V74A2 had larger *B*-factors than those of V74A (Figure 4j).

The crystal structures in the vicinity of the mutation sites are illustrated in Figure 5. V93A, V100A, V125A, and V130A were substituted in the interior of the protein, and the residues around the mutation site shifted toward the created cavity (Figure 5c, e, h, and i). These shifts have

Table 2: Thermodynamic Parameters for Denaturation of Mutant Human Lysozymes (Val→Ala) at Different pHs

protein	pH	T_d (°C)	ΔH_{cal} (kJ/mol)	ΔH_{vH} (kJ/mol)	ratio $\Delta H_{cal}/\Delta H_{vH}$	ΔC_p [a] (kJ/mol K)
V2A	3.17	68.7	490	502	0.98	7.0
	2.88	63.7	464	473	0.98	6.7
	2.71	60.3	439	456	0.96	6.4
	2.55	57.6	418	431	0.97	4.5
					0.97	6.2 ± 1.4
V74A	2.88	67.1	490	510	0.96	6.6
	2.71	64.1	469	502	0.94	5.6
	2.55	61.0	452	481	0.94	6.4
					0.94	6.2 ± 0.7
V93A	3.17	71.1	502	531	0.95	7.4
	3.02	68.3	490	523	0.94	4.4
	3.02	68.6	494	527	0.94	3.8
	2.88	66.1	473	510	0.93	4.4
	2.71	62.6	448	494	0.91	4.6
	2.55	59.8	435	464	0.94	4.9
					0.94	4.9 ± 1.4
V99A	3.02	67.8	481	506	0.95	6.4
	2.88	65.2	464	490	0.95	4.6
	2.71	62.1	448	469	0.96	6.3
	2.55	59.2	423	448	0.94	6.1
					0.95	5.9 ± 1.0
V100A	3.17	72.1	490	536	0.91	4.7
	3.02	69.9	485	540	0.90	3.3
	2.71	64.3	456	498	0.92	4.5
	2.55	61.5	448	477	0.94	4.3
					0.92	4.2 ± 0.8
V110A	3.02	71.2	515	540	0.95	5.8
	2.88	69.7	510	540	0.94	4.6
	2.71	66.5	494	527	0.94	4.1
	2.55	63.8	477	498	0.96	4.6
					0.95	4.8 ± 0.9
V121A	3.17	69.9	490	494	0.99	5.8
	2.88	64.2	456	469	0.97	6.7
	2.71	60.5	435	448	0.97	4.9
	2.55	57.4	410	427	0.96	6.6
					0.97	6.0 ± 1.0
V125A	3.17	69.6	498	515	0.97	4.6
	2.88	64.3	469	494	0.95	4.8
	2.71	61.0	452	460	0.98	6.3
	2.55	58.1	435	448	0.97	4.3
	2.55	58.0	435	444	0.98	4.8
					0.97	5.0 ± 0.9
V130A	3.17	70.6	502	531	0.95	3.6
	3.02	68.0	485	523	0.93	3.2
	2.88	65.7	469	510	0.92	4.6
	2.71	62.4	452	481	0.94	6.7
	2.55	59.6	435	464	0.94	7.0
					0.94	5.0 ± 2.0

[a] ΔC_p was obtained from each calorimetric curve.

Table 3: Thermodynamic Parameters for Denaturation of Val Mutant Human Lysozymes at the Denaturation Temperature (64.9 °C) of the Wild-Type Protein at pH 2.7

protein	T_d (°C)	ΔT_d (°C)	ΔC_p [a] (kJ/mol K)	ΔH_{cal} (kJ/mol)	$\Delta\Delta G$ (kJ/mol)	$\Delta H_{cal}/\Delta H_{vH}$
wild-type[b]	64.9 ± 0.5		6.6 ± 0.5	477 ± 4	(0)	0.95
V2A	60.3 ± 0.2	−4.6	6.5 ± 0.5	468 ± 4	−6.3 ± 0.2	0.98
V74A	63.8 ± 0.1	−1.1	6.2 ± 0.4	476 ± 2	−1.5 ± 0.2	0.95
V93A	62.6 ± 0.2	−2.3	6.4 ± 0.4	466 ± 4	−3.1 ± 0.3	0.93
V99A	61.9 ± 0.02	−3.0	6.6 ± 0.5	463 ± 3	−4.1 ± 0.1	0.95
V100A	64.1 ± 0.2	−0.8	4.2 ± 0.4	461 ± 3	−1.1 ± 0.3	0.92
V110A	66.4 ± 0.4	+1.5	5.2 ± 0.4	484 ± 2	+2.2 ± 0.6	0.95
V121A	60.4 ± 0.2	−4.5	6.4 ± 0.3	460 ± 3	−6.0 ± 0.3	0.98
V125A	60.9 ± 0.1	−4.0	5.4 ± 0.1	472 ± 0.5	−5.5 ± 0.1	0.97
V130A	62.3 ± 0.1	−2.6	6.3 ± 0.6	464 ± 5	−3.5 ± 0.1	0.93

[a] ΔC_p was obtained from the slope of ΔH against T_d. [b] Takano et al. (1995).

Table 4: X-ray Data Collection and Refinement Statistics for Val Mutant Human Lysozymes

	V2A	V74A	V93A	V99A	V100A	V110A	V121A	V125A	V130A	V74A2[a]
A. Data Collection										
cell dimension (Å)										
a	57.09	56.64	56.65	56.73	56.56	56.80	56.77	56.70	56.67	56.61
b	61.23	61.01	60.85	61.09	61.00	60.91	60.92	61.12	60.92	61.01
c	33.60	33.77	33.86	33.92	33.70	33.83	33.82	33.76	33.83	33.79
resolution (Å)	1.8	1.8	1.8	1.8	1.8	1.8	1.8	1.8	1.8	1.8
no. of measd reflcns	34 394	35 925	36 666	35 708	33 859	34 707	35 004	36 385	35 420	34 497
no. of ind. reflcns	10 331	10 631	11 122	10 408	10 366	10 973	10 733	10 428	10 910	10 843
completeness of data (%)	90.0	93.2	98.0	91.1	91.3	95.9	94.0	91.3	95.7	95.6
$I/\sigma I$ (1.9−1.8 Å)	5.5	9.2	9.1	6.4	4.9	6.9	5.2	7.0	6.0	4.9
R merge (%)[b]	5.4	3.7	4.0	5.1	5.1	3.4	4.6	4.6	5.3	6.8
B. Refinement										
no. of atoms	1181	1228	1237	1220	1203	1234	1216	1192	1243	1208
no. of solvent atoms	154	201	210	193	176	207	189	165	216	181
resolution range (Å)	8−1.8	8−1.8	8−1.8	8−1.8	8−1.8	8−1.8	8−1.8	8−1.8	8−1.8	8−1.8
no. of reflcns used	9 945	10 311	10 827	10 036	9 912	10 504	10 313	10 148	10 504	10 407
completeness of data (%)	88.2	92.1	96.8	89.1	88.8	93.6	92.0	90.4	93.8	93.0
R factor[c]	0.173	0.160	0.159	0.168	0.160	0.153	0.154	0.158	0.158	0.170
rmsd bond (Å)	0.009	0.008	0.008	0.009	0.009	0.008	0.009	0.008	0.008	0.008
rmsd angle (deg)	1.52	1.49	1.51	1.50	1.50	1.49	1.53	1.50	1.51	1.50
mean *B* (Å^2)										
main-chain	17.0	13.3	13.0	13.8	14.6	13.6	14.5	14.7	13.2	14.9
side-chain	22.1	17.7	17.4	18.7	19.3	18.3	19.2	19.2	17.5	19.4

[a] This is the same protein as V74A and is obtained from a smaller crystal as a reference to estimate the errors in the structure. [b] R merge $= 100\sum|I_{h,i} - \langle I_h\rangle|/\sum I_{hi}$. $I_{h,i}$ are individual values, and $\langle I_h\rangle$ is the mean value of the intensity of reflection h. [c] R factor $= \sum||F_o| - |F_c||/\sum|F_o|$.

not been observed in the Ile to Val mutant lysozymes (Takano et al., 1995). These shifts may be caused by creation of a larger cavity due to the deletion of two methylene groups or by an increase in the flexibility of the main-chain due to the substitution with Ala. The Val to Ala mutants examined did not contain any solvent molecules in the cavities, although this has been observed in one Ile mutant (Takano et al., 1995).

(i) V93A, V99A, and V100A Substitutions in the α-Helix in the Interior of a Protein. Val93, 99, and 100 are all located in an α-helix (residues 90−100) in the center of the protein and have small side-chain solvent accessible surface areas. For V93A, the Leu15 and Met17 residues facing the side-chain of Val93 shifted toward the created cavity without movement of the mutated residue which is in the center of the α-helix (Figure 5c). The largest shift in the vicinity of Ala93 was 0.7 Å for the sulfur atom of Met17. In contrast, V100A substituted at the edge of the α-helix underwent a shift of Ala100 itself toward the cavity (Figure 5c) and the loop regions (residues 101−109) (Figure 3e) followed. The C_β atom of Ala100 moved 0.8 Å, and some main-chain atoms in residues 101−109 moved 0.4 Å. The mutation of Val99, whose side-chain was sandwiched between Trps (64 and 109), resulted in shifts and an increase in *B*-factors in the following loop region (Figures 3d and 4d). The substitutions in this α-helix (residues 90−100) mainly affected the surrounding residues.

(ii) V121A, V125A, and V130A Substitutions in the C-Terminal Region of a Protein. The changes in structure for V121A, V125A, and V130A were quite different, although Val121 and Val125 have similar ASA values in the β-turn. When Val121 was replaced by Ala, the movements were smaller than those of the other mutant proteins (Figures 3g and 5g). The average of the rms differences for the main-chain atoms between V121A and the wild-type was 0.08 Å. V125A had structural changes in the residues in the C-terminal region (residues 119−130) due to the movement of Ala125 toward the created cavity (Figures 3h and 5h). The maximal shift (0.7 Å) of the main-chain atoms was for the C_α atom of Gln126. The movements of V130A were largely observed only in residues 129 and 130 (Figures 3i and 5i). The rms differences for the main-chains of the residues 129 and 130 were 0.5 and 1.4 Å, respectively.

(iii) V2A, V74A, and V110A Substitutions on the Surface of a Protein. The deletions of the methylene groups on the surface of the protein allowed water molecules to move closer

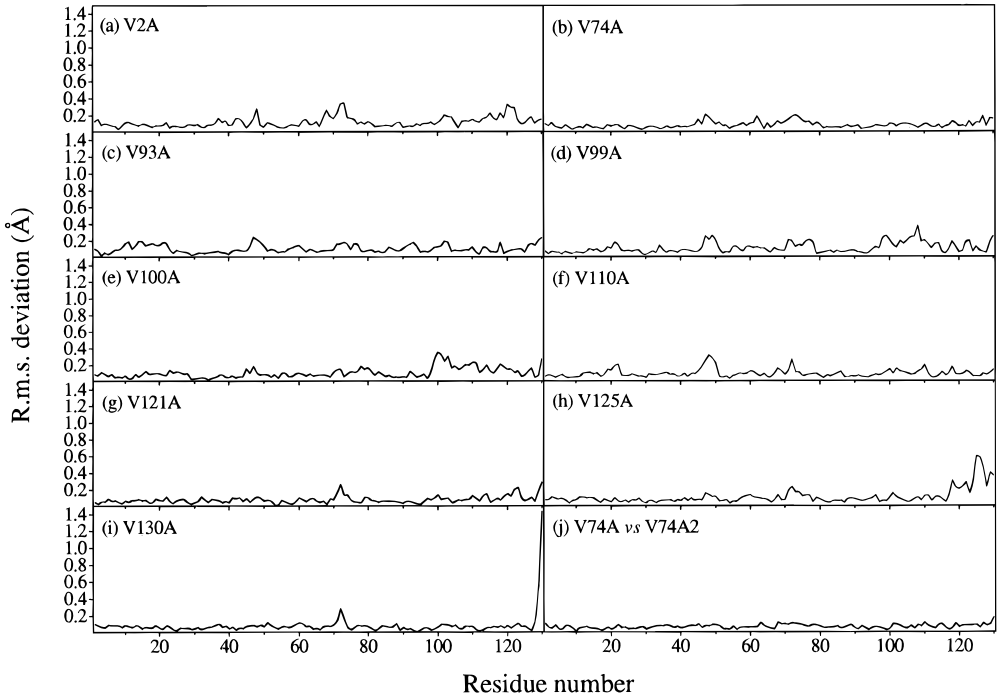

FIGURE 3: RMSDs for the main-chain atoms between each mutant and the wild-type structure after a least-squares fit of both structures, using the main-chain atoms (a−i) and those between V74A and V74A2 as a reference (j). Panels a−i represent V2A, V74A, V93A, V99A, V100A, V110A, V121A, V125A, and V130A, respectively.

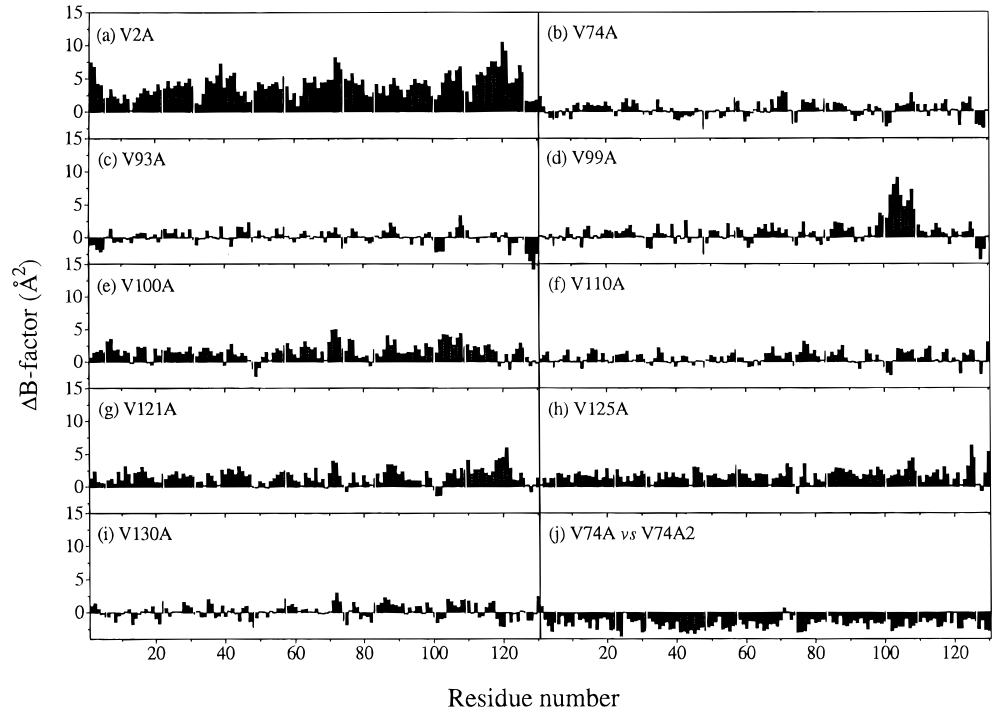

FIGURE 4: The differences in the *B*-factors of each residue for the main-chain atoms between each mutant and the wild-type structure (a−i) and those between V74A and V74A2 as a reference (j). Panels a−i represent V2A, V74A, V93A, V99A, V100A, V110A, V121A, V125A, and V130A, respectively.

to the protein molecule (Figure 5b and f). Between the two V74A structures (V74A and V74A2), the water molecules ordered on the first hydration phase surrounding the mutation site were identical, but when they were ordered in a second phase, they varied.

DISCUSSION

The changes in the thermodynamic properties for the denaturation of the Val to Ala mutants of human lysozyme differed considerably (Table 3). Our primary goal is to understand the observed differences. The changes in the structures of Val to Ala mutant lysozymes were also different (Figure 5). We examined the correlations between the changes in the thermodynamic parameters of the denaturation and the following structural features of the proteins: (i) the structural characteristics at each mutation site in the wild-type structure, (ii) the structural differences at each mutation site between the wild-type and the mutant structures and (iii)

the structural differences throughout the whole structures between the wild-type and the mutant structures, including five Ile to Val mutants of human lysozyme (Takano et al., 1995). For mutant proteins in which methylene groups have been removed, the thermodynamic parameters for denaturation should depend on structural characteristics of the protein, such as accessible surface area (ASA) (Pace, 1992), packing density (Serrano et al., 1992), and cavity volume (Eriksson et al., 1992).

In addition, the strain due to a Val side-chain in the native protein may be relieved in the Ala mutant. The conformation of Val residues in the wild-type structure are listed at Table 1. Although the χ_1 value of Val74 deviates from the low-energy minima (Zimmerman et al., 1977), its side-chain is highly exposed and flexible: the *B*-factors for the side-chain were larger than those of other Val side-chains. Therefore, Val74 has little strain. No unfavorable side-chain conformations of the Val residues were found in the present studies.

Correlation of $\Delta\Delta G$ *with Accessible Surface Area (ASA) of Each Substituted Residue*. Pace (1992) has suggested that values of $\Delta\Delta G$ of hydrophobic mutant proteins could be corrected to the same accessibility, namely, 100% buried. For six proteins, the average $\Delta\Delta G$ values, which are divided by the fraction buried for the side-chain in the wild-type proteins, of 15 Val to Ala and 20 Ile to Val mutants are 10.7 and 4.6 kJ/mol, respectively (Pace et al., 1996). These values are similar to ΔG_{tr} from cyclohexane, 9.3 for Val → Ala and 3.7 for Ile → Val (Pace, 1995; Radzika & Wolfenden, 1988). In case of the human lysozyme, the average corrected $\Delta\Delta G$ values were decidedly lower than other results, 4.3 for Val → Ala and 3.3 for Ile → Val, except for V2A, V74A, and V110A the residues of which are quite accessible to the solvent. These values are more similar to the ΔG_{tr} values from octanol, 5.2 for Val → Ala and 3.3 for Ile → Val, than those from cyclohexane (Fauchere & Pliska, 1983). The reason for this is probably that the unfolded state for human lysozyme is less accessible to the solvent, mainly due to the 4 disulfide bonds in human lysozyme, than for most of the other proteins that have been used in similar studies (Pace et al., 1990, 1992).

Figure 6a shows the relation between the accessible surface area (%) of the side-chain for each mutation residue in the wild-type structure and the denaturation Gibbs energy changes. However, we did not find good correlation between them. We then tried to calculate the changes in ASA value using the mutant protein structures.

Correlation of $\Delta\Delta G$ *with Changes in Hydrophobic Surface Area Exposed upon Denaturation (*$\Delta\Delta ASA_{HP}$*)*. The ASA values of the Val residues in human lysozyme varied from 0 to 75% (Table 1). We estimated the changes in hydrophobic surface area exposed upon denaturation ($\Delta\Delta ASA_{HP}$) using the following equation, where $\Delta\Delta ASA_{HP}$ is measure of the changes in hydrophobic surface area exposed upon denaturation.

$$\begin{aligned}\Delta\Delta ASA_{HP} &= (\Delta ASA_{mutant})_{HP} - (\Delta ASA_{wild})_{HP} \\ &= [(ASA^{extended})_{mutant} - (ASA^{fold})_{mutant}]_{HP} - \\ &\qquad [(ASA^{extended})_{wild} - (ASA^{fold})_{wild}]_{HP} \\ &= [(ASA^{extended})_{mutant} - (ASA^{extended})_{wild}]_{HP} - \\ &\qquad [(ASA^{fold})_{mutant} - (ASA^{fold})_{wild}]_{HP} \quad (4)\end{aligned}$$

$ASA^{extended}$ was calculated using the actual polypeptide with extended conformation (Oobatake & Ooi, 1993). Yu et al. (1995) have observed a strong relationship between $\Delta\Delta ASA$ based on the wild-type structure and the changes in the Gibbs energy of the unfolding for mutations in BPTI. We estimated $\Delta\Delta ASA_{HP}$ values in three ways: two of them are values for just the substituted residue, but the other is for all hydrophobic residues. The $\Delta\Delta ASA_{HP}$ values in Figure 6b−d represent the difference between the ΔASA for each substituted residue using the wild-type structure and that using the model mutant structure deleting the methylene groups based on the coordinates of the wild-type structure (model), the difference between ΔASA values for each substituted residue using the wild-type and the mutant structure, and the difference between the ΔASA for all of the hydrophobic residues using the wild-type and the mutant structure, respectively. In most reports [e.g., Jackson et al. (1993), Yu et al. (1995), and Tamura and Sturtevant (1995)], wild-type structures are used for evaluation of ΔASA for mutant proteins like that in Figure 6b. The $\Delta\Delta ASA_{HP}$ values in Figure 6b and 6c were essentially the same, indicating that the conformational changes at the substitution sites are not large enough to affect the ASA values. However, the correlations between $\Delta\Delta ASA_{HP}$ and $\Delta\Delta G$ were poor. The relationship of $\Delta\Delta G$ and $\Delta\Delta ASA_{HP}$ of all of the hydrophobic residues showed less scatter from the line (dotted) expected from the transfer Gibbs energy of a methylene group (Figure 6d) than those with the $\Delta\Delta ASA_{HP}$ of each substituted residue (Figure 6c). These results suggest that the substitutions involve structural rearrangements of the overall structure, which affect the stabilities, and confirm structural changes of residues far from substitution sites (Figure 3).

We should note that the data points were scattered on the expected line as shown in Figure 6a−d, suggesting that other factors also affected the conformational stability. Residues exposed on the surface of a protein will have little interaction with other residues. At positions Val2, Val74, and Val110, the side-chains were highly exposed, however, the $\Delta\Delta G$ values were −6.3, −1.5, and +2.2 kJ/mol, respectively. Because Val2, Val74, and Val110 are located on the β-sheet, long loop, and α-helix, respectively, the difference in stability among them may depend on the secondary structure at the substitution site. Table 5 lists the $\Delta\Delta G$ values measured by DSC and the $\Delta\Delta G$ expected from the hydrophobicity corrected for ASA values of each substitution (Fauchere & Pliska, 1983; Pace, 1992). As shown in Table 5, for the substitutions of Val by Ala on the α-helix, the Gibbs energy changes are smaller than the expected values. The secondary structure propensities of Val and Ala are different: the ranking in an α-helix is Ala > Val, and the ranking in a β-sheet is Val > Ala (Chou & Fasman, 1978). The stabilities of proteins substituted in an α-helix (Dao-Pin et al., 1990; Serrano et al., 1992; Blaber et al., 1993; Pinker et al., 1993) and in a β-sheet (Kim & Berg, 1993; Smith et al., 1994; Minor & Kim, 1994; Otzen & Fersht, 1995) have been examined. For most of them, the ranking of the stabilities is coincident with the ranking of the secondary structure propensities of Chou and Fasman (1978). In the present case, data over the expected line (the dotted line) in Figure 6a−d might contain the influence of the secondary structure propensities. When the mutants on non-secondary structures were considered, the correlation between $\Delta\Delta G$ and $\Delta\Delta ASA_{HP}$ had a correlation coefficient of 0.88 for seven points (V74A, V121A, V125A, I23V, I56V, I89V, and I106V), as shown

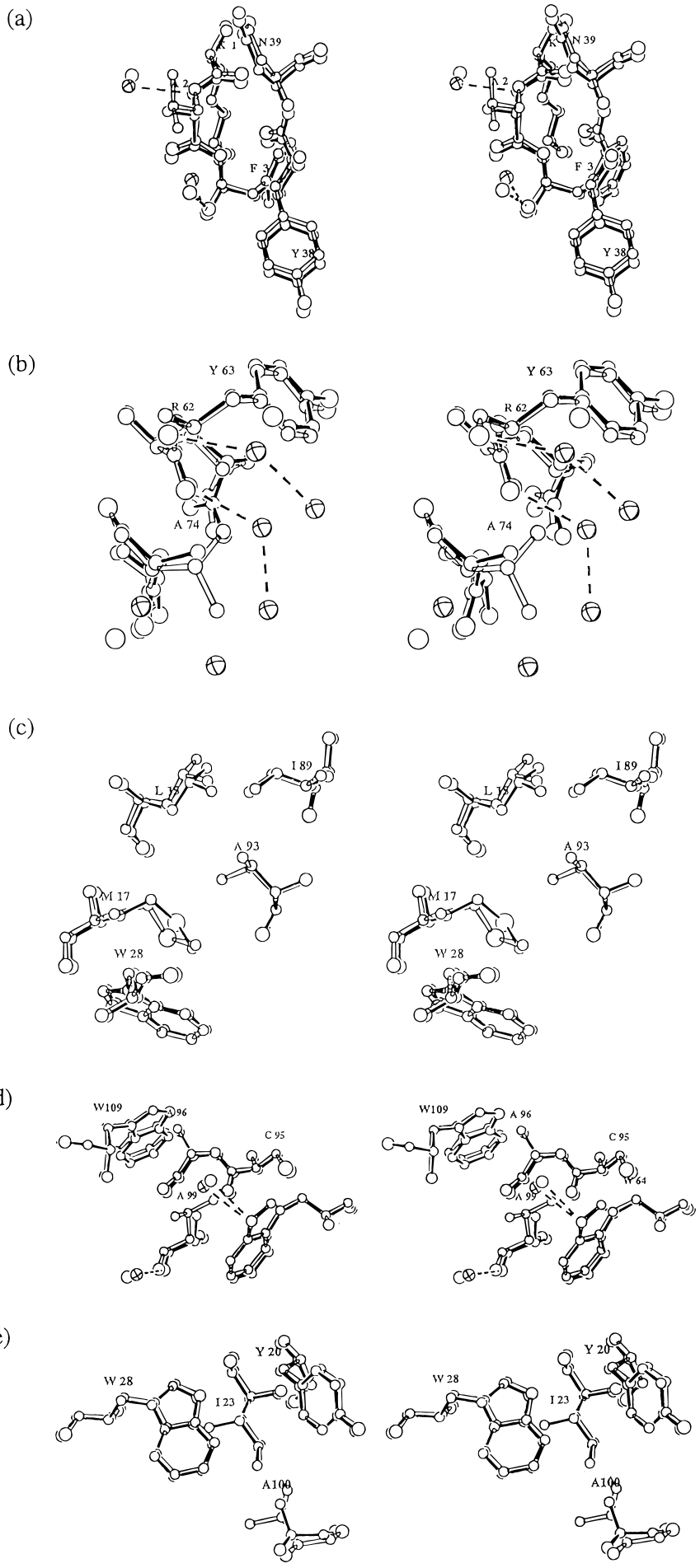
(a)
N 39
F 3
Y 38
(b)
Y 63
R 62
A 74
(c)
I 89
A 93
M 17
W 28
(d)
W109
A 96
C 95
A 99
(e)
Y 20
W 28
I 23
A100

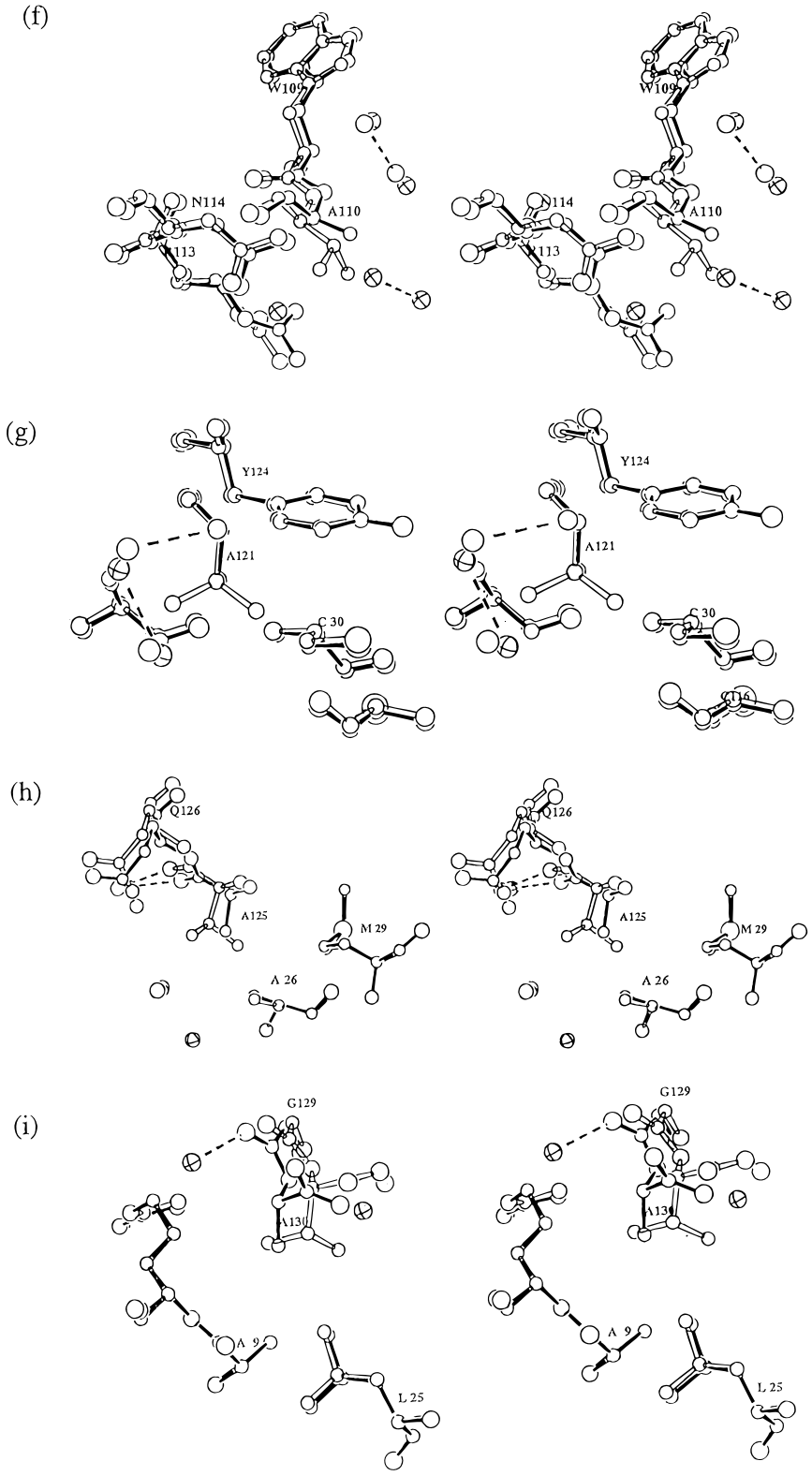

FIGURE 5: Stereodrawings (Johnson, 1976) showing the structure in the vicinity of the mutation sites. The wild-type (open bonds) and mutant structures (filled bonds) are superimposed. Panels a−i represent V2A, V74A, V93A, V99A, V100A, V110A, V121A, V125A, and V130, respectively. Solvent water molecules are drawn as open circles (wild-type) and crossed circles (mutants). The broken lines indicate hydrogen bonds.

by the continuous line in Figure 6d. A similar analysis of the mutants on the α-helices showed a very good correlation with the correlation coefficients of 0.95 for four points (V93A, V99A, V100A, and V110A), as shown by the broken line in Figure 6d. In this connection, the correlation coefficients of all data for Figure 6c and 6d were only 0.22 and 0.37, respectively. These results indicate that the secondary structure propensities of the amino acid residues in α-helices compensated for the destabilization due to the removal of the methylene groups and also that the α-helix propensity corrections may apply at completely buried sites if there is no steric strain as in this study. Thus, V110A was more stable than the wild-type protein because the increment in stabilization due to helix propensity was greater

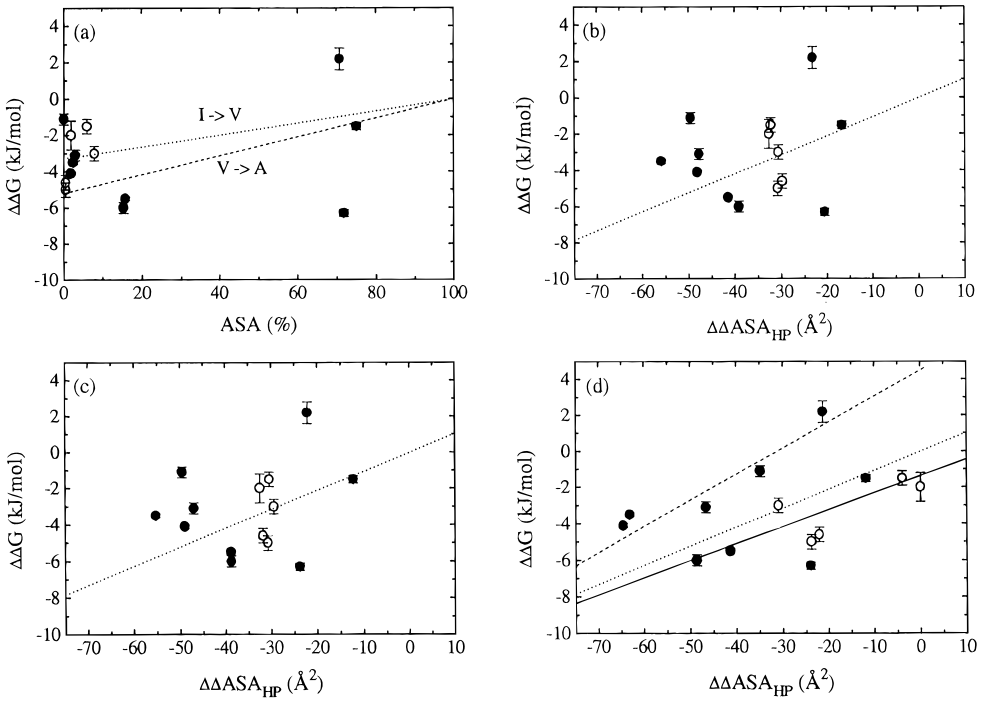

FIGURE 6: Correlation of accessible surface area (ASA) or changes in hydrophobic surface area exposed upon denaturation ($\Delta\Delta ASA_{HP}$) with the thermodynamic parameters of denaturation for the mutant proteins at 64.9 °C ($\Delta\Delta G$). Val → Ala mutants are shown as solid circles and Ile → Val as open circles. (a) $\Delta\Delta G$ and the accessible surface area (ASA) (%) of the substituted residue in the wild-type structure. The broken (Val → Ala) and dotted (Ile → Val) lines show the values estimated from the transfer Gibbs energy of a hydrophobic group from n-octanol to water (Fauchere & Pliska, 1983). (b) $\Delta\Delta G$ and the difference in ΔASA for each substituted residue calculated using just the wild-type structure with the mutant structure modeled by deleting the methylene groups from the coordinates of the wild-type structure. (c) $\Delta\Delta G$ and the difference in ΔASA for each substituted residue calculated using both the wild-type and the mutant structure. (d) $\Delta\Delta G$ and the difference in ΔASA for all of the hydrophobic residues calculated using the wild-type and the mutant structure. The continuous and broken lines show the linear regression of the mutant protein on the non-secondary structures (V74A, V121A, V125A, I23V, I56V, I89V, and I106V) and the mutants on the α-helices (V93A, V99A, V100A, and V110A), respectively. The dotted lines in b−d indicate the values expected from the transfer (Gibbs energy of a methylene group (0.11 kJ/mol Å^2) (Fauchere & Pliska, 1983; Connolly, 1983, 1993).

Table 5: Comparison of Measured $\Delta\Delta G$ with $\Delta\Delta G$ Expected from Hydrophobicity Corrected Using the ASA Value of Each Substitution Residue for Val and Ile Mutant Human Lysozymes (in kJ/mol)

mutant	position of substitution	measd $\Delta\Delta G$ (A)	expected $\Delta\Delta G^a$ (B)	discrepancy ($A-B$)
V93A	α-helix	−3.1	−5.0	+1.9
V99A	α-helix	−4.1	−5.1	+1.0
V100A	α-helix	−1.1	−5.2	+4.1
V110A	α-helix	+2.2	−1.5	+3.7
V2A	β-sheet	−6.3	−1.5	−4.8
V121A	β-turn[b]	−6.0	−4.4	−1.6
V125A	β-turn[b]	−5.5	−4.4	−1.1
V74A		−1.5	−1.3	−0.2
V130A	C-terminal	−3.5	−5.1	+1.6
I59V	β-sheet	−4.6	−3.3	−1.3
I23V	β-turn[b]	−1.5	−3.1	+1.6
I56V	β-turn[b]	−5.0	−3.3	−1.7
I106V	β-turn[b]	−3.0	−3.0	0
I89V		−2.0	−3.2	+1.2

[a] These were calculated using the transfer Gibbs energy from *n*-octanol to water (Fauchere & Pliska, 1983). When fully buried, $\Delta\Delta G$ of Val → Ala and Ile → Val are −5.2 and −3.3 kJ/mol, respectively. ASA (%) of Ile residues (23, 56, 59, 89, and 106) calculated in the same way as Val residues (in Table 1) are 6.0, 0.5, 0.5, 1.9, and 3.9, respectively. [b] Defined by Rose et al. (1985).

than the small decrease in stability due to the removal of methylene groups located largely on the protein surface. In contrast, V2A was less stable than expected due to the unfavorable β-sheet propensity. It has been reported that α-helix propensity and β-sheet propensity contribute 2.3 and −3.8 kJ/mol to the stability of Val to Ala substitutions (Pace, 1995).

The mutant proteins with similar measured $\Delta\Delta G$ and expected $\Delta\Delta G$ values were V74A and I106V (Table 5). The discrepancy was also small for V99A, V125A, I59V, and I89V. V74A (Figure 3b), I89V, and I106V (Takano et al., 1995) are the mutant proteins with the smallest structural changes. These results suggest that $\Delta\Delta G$ correlates with the ASA value corrected for the accessibility, if the structure is not affected by the substitution and the substitution site is not located in the secondary structure.

Correlation of $\Delta\Delta G$ with Cavity Volume and with Packing Density. Eriksson et al. (1992, 1993) have found the relationship between the created cavity volume and $\Delta\Delta G$ in Leu → Ala and Phe → Ala mutant T4 lysozymes:

$$\Delta\Delta G = \Delta\Delta G_{tr} + \Delta\Delta G_{cav} + \Delta\Delta G_{other} \qquad (5)$$

where $\Delta\Delta G_{tr}$ is the difference in the hydrophobicity of the amino acids, $\Delta\Delta G_{cav}$ is an energy component that depends on the size of the cavity created by substitution and $\Delta\Delta G_{other}$ represents other energy terms that may result from differences in the side-chain rotamer angles, differences in the side-chain conformational entropy, differences in the bond angles and bond lengths, and any other differences between the structures of the wild-type and the mutant proteins. For barnase, the correlation between $\Delta\Delta G$ and cavity volume has not been seen in Ile → Val mutants (Buckle et al., 1993), but in Ile → Ala mutants there is an approximately linear relationship

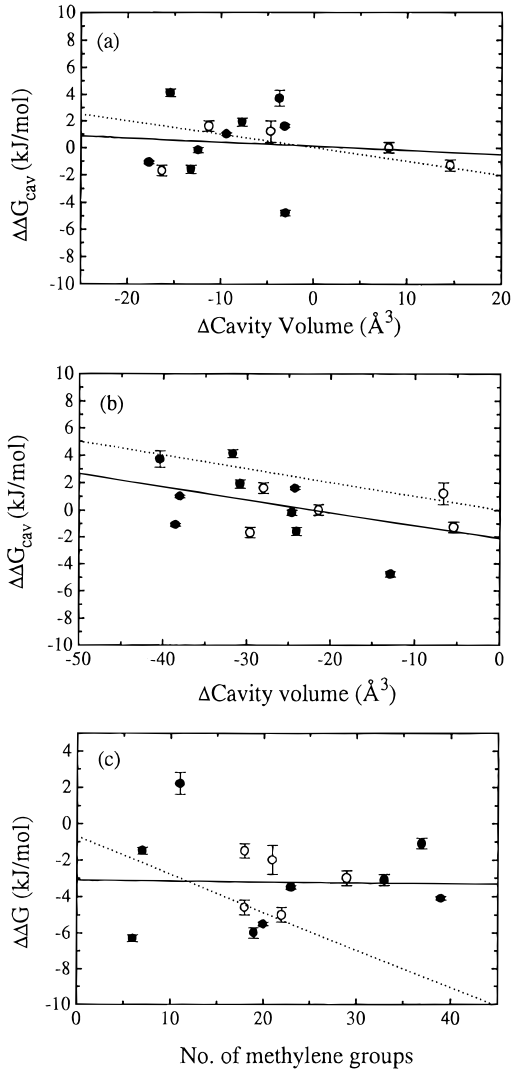

FIGURE 7: Correlation of cavity volume and packing density with the thermodynamic parameters of denaturation for the mutant proteins. Val → Ala mutants are shown as solid circles and Ile → Val as open circles. The continuous lines show the linear regression of all the proteins. (a) $\Delta\Delta G_{cav}$ (= $\Delta\Delta G$ − $\Delta\Delta G_{tr}$) and the difference in the total cavity volume between each mutant protein and the wild-type structure using the probe size 1.20 Å (Connolly, 1983, 1993). (b) $\Delta\Delta G_{cav}$ (= $\Delta\Delta G$ − $\Delta\Delta G_{tr}$) and the difference in the total cavity volume between each mutant protein and the wild-type structure using the probe size 1.40 Å (Connolly, 1983, 1993). The $\Delta\Delta G_{tr}$ values in a and b are corrected by the accessibility of each residues. The dotted lines in a and b indicate the values proposed by Eriksson et al. (1992). (c) $\Delta\Delta G$ and the packing density (number of methylene groups within 6 Å of the removed atoms). The dotted line shows the best fit of the barnase and chymotrypsin inhibitor 2 data to a linear equation obtained by Otzen et al. (1995).

between them (Buckle et al., 1996). Five Ile mutant human lysozymes have shown some correlation with the line derived by Eriksson et al. (1992) for the changes in the total cavity volume and $\Delta\Delta G$ (Takano et al., 1995).

We have determined the size of the cavities in the Val mutant crystal structures using the procedure of Connolly (1985, 1993) with a probe radius of $r = 1.20$ Å. The reason for using this program and this probe size was to allow comparison with previous reports (Eriksson et al., 1992, 1993; Takano et al., 1995). The van der Waals radii of the atoms in the new version of the Connolly procedure are improved compared to those used in the previous study

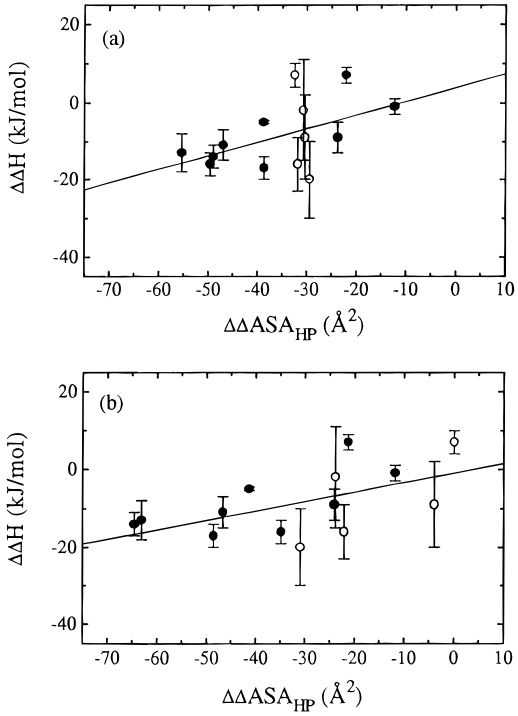

FIGURE 8: Correlation of changes in hydrophobic surface area exposed upon denaturation ($\Delta\Delta ASA_{HP}$) with enthalpy changes of denaturation for the mutant proteins at 64.9 °C ($\Delta\Delta H$). Val → Ala mutants are shown as solid circles and Ile → Val as open circles. The continuous lines show the linear regression of all the proteins. (a) $\Delta\Delta H$ and the difference in ΔASA for each substituted residue using the wild-type and the mutant structure (correlation coefficient = 0.49). (b) $\Delta\Delta H$ and the difference in ΔASA for all of the hydrophobic residues using the wild-type and the mutant structure (correlation coefficient = 0.56).

(Takano et al., 1995). The cavity volumes of Ile mutants were also recalculated for comparison.

A cavity at each mutation site of Val to Ala mutants of human lysozyme was not detected, except for V93A, indicating that the cavity size became smaller than the probe radius or that the probe connected with the protein surface. Therefore, we also calculated the cavity volume of each model structure obtained by the deletion of the methylene groups from the coordinates of the wild-type structure (model). However, the cavity volume could again only be calculated for model-V93A. The detected cavity volume of V93A and model-V93A corresponded to one deleted methylene group. Next, we tried calculations using smaller probe radii of 1.15, 1.10, 1.05, and 1.00 Å. For these smaller probe radii, V99A, V100A, model-V99A, and model-V100A had cavities which were equivalent to one methylene group. These results indicate that it is difficult to determine the cavity volume of these mutant proteins with Val → Ala mutations.

Figure 7a and 7b shows the correlation between $\Delta\Delta G_{cav}$ (= $\Delta\Delta G$ − $\Delta\Delta G_{tr}$) and the total cavity volume changes between the wild-type and the mutant proteins for the probe sizes 1.20 and 1.40 Å which is typically assumed to be the radius of a water molecule. Here, the $\Delta\Delta G_{tr}$ values were corrected for the accessibility of each residue. The correlations between them were poor, but these results show that cavity detection was highly dependent on the probe radius (Hubbard & Argos, 1995).

The $\Delta\Delta G$ values for mutations in the hydrophobic core of chymotrypsin inhibitor 2 correlate with the packing density

(the number of methylene groups within 6 Å of the removed atoms) (Jackson et al., 1993), and the partly exposed minicore correlates with a mixture of the ASA and the packing density (Otzen et al., 1995). In the case of the human lysozyme mutants, the correlation between the packing density and $\Delta\Delta G$ is shown in Figure 7c. The correlation with only the mutants in the interior of the protein was poor, and the data were far from the dotted line in Figure 7c obtained from barnase and chymotrypsin inhibitor 2 (Otzen et al., 1995).

Correlation of ΔH *with* $\Delta\Delta ASA_{HP}$. There are only a few data on the differences in the enthalpy changes ($\Delta\Delta H$) between wild-type and mutant proteins. One reason may be the large error in measurements for ΔH. As described in our previous paper (Takano et al., 1995), to minimize the error we measured at several pHs for each protein and determined the thermodynamic parameters at the temperature (near 65 °C) where the ΔH values were obtained directly by the measurements. The plots of T_d vs ΔH (not shown) indicate the obvious differences between proteins.

No attempt has been made previously to correlate $\Delta\Delta H$ values with changes in the accessibility of mutant proteins. Makhatadze and Privalov (1995) have estimated that the enthalpy change ($\Delta H^{vdW} + \Delta H^{hyd}$) of nonpolar atoms at 65 °C using a model compound is 80 J/mol Å^2. The correlation between the denaturation enthalpies of the mutant human lysozymes and $\Delta\Delta ASA_{HP}$ of each mutation site is shown in Figure 8a. The comparison with the total structural changes including the Ile mutant lysozymes (Figure 8b) showed better correlation than with the local ones. However, the correlation coefficient is still low (0.56). This suggests that other factors which are particular for each position of a protein also affect the enthalpy change of denaturation.

ACKNOWLEDGMENT

We thank Professor Nick Pace (Texas A&M University) for helpful advice and useful discussions. We also thank Takeda Chemical Ind., Ltd. (Osaka), for providing plasmid pGEL125 and Takara Shuzo Co., Ltd. (Kyoto), for the mass spectrum measurements of the mutant proteins.

REFERENCES

Blaber, M., Zhang, X. J., & Matthews, B. W. (1993) *Science 260*, 1637−1640.
Brunger, A. T. (1992) X-PLOR Manual, Ver. 3.1, Yale University, New Haven, CT.
Buckle, A. M., Henrick, K., & Fersht, A. R. (1993) *J. Mol. Biol. 234*, 847−860.
Buckle, A. M., Cramer, P., & Fersht, A. R. (1996) *Biochemistry 35*, 4298−4305.
Chou, P. Y., & Fasman, G. D. (1978) *Adv. Enzymol. 47*, 45−148.
Connolly, M. L. (1985) *J. Am. Chem. Soc. 107*, 1118−1124.
Connolly, M. L. (1993) *J. Mol. Graphics 11*, 139−141.
Dao-Pin, S., Baase, W. A., & Matthews, B. W. (1990) *Proteins: Struct., Funct., Genet. 7*, 198−204.
Eriksson, A. E., Baase, W. A., Zhang, X.-J., Heinz, D. W., Blaber, M., Baldwin, E. P., & Matthews, B. W. (1992) *Science 255*, 178−183.
Eriksson, A. E., Baase, W. A., & Matthews, B. W. (1993) *J. Mol. Biol. 229*, 747−769.
Fauchere, J.-L., & Pliska, V. (1983) *Eur. J. Med. Chem. 18*, 369−375.
Herning, T., Yutani, K., Inaka, K., Kuroki, R., Matsushima, M., & Kikuchi, M. (1992) *Biochemistry 31*, 7077−7085.
Hubbard, S. J., & Argos, P. (1995) *Protein Eng. 8*, 1011−1015.
Jackson, S. E., Moracci, M., elMasry, N., Johnson, C. M., & Ferhst, A. R. (1993) *Biochemistry 32*, 11259−11269.
Johnson, C. K. (1976) ORTEPII: A Fortran thermalellipsoid plot program for crystal structure illustration, Oak Ridge National Laboratory, TN.
Kauzmann, W. (1959) *Adv. Protein Chem. 14*, 1−63.
Kellis, J. T., Jr. Nyberg, K., Sali, D., & Fersht, A. R. (1988) *Nature 333*, 784−786.
Kellis, J. T., Jr. Nyberg, K., & Fersht, A. R. (1989) *Biochemistry 28*, 4914−4922.
Kim, C. A., & Berg, J. M. (1993) *Nature 362*, 267−270.
Kraulis, P. J. (1991) *J. Appl. Crystallogr. 24*, 946−950.
Kuroki, R., Inaka, K., Taniyama, Y., Kidokoro, S., Matsushima, M., Kikuchi, M., & Yutani, K. (1992a) *Biochemistry 31*, 8323−8328.
Kuroki, R., Kawakita, S., Nakamura, H., & Yutani, K. (1992b) *Proc. Natl. Acad. Sci. U.S.A. 89*, 6803−6807.
Makhatadze, G. I., & Privalov, P. L. (1995) *Adv. Protein Chem. 47*, 307−429.
Matsumura, M., Becktel, W., & Matthews, B. W. (1988) *Nature 334*, 406−410.
Matthews, B. W. (1993) *Annu. Rev. Biochem. 62*, 139−160.
Minor, D. L., & Kim, P. S. (1994) *Nature 367*, 660−663.
Oobatake, M., & Ooi, T. (1993) *Prog. Biophys. Mol. Biol. 59*, 237−284.
Otzen, D. E., & Fersht, A. R. (1995) *Biochemistry 34*, 5718−5724.
Otzen, D. E., Rheinnecker, M. E., & Fersht, A. R. (1995) *Biochemistry 34*, 13051−13058.
Pace, C. N. (1992) *J. Mol. Biol. 226*, 29−35.
Pace, C. N. (1995) *Methods Enzymol. 259*, 538−554.
Pace, C. N., Laurents, D. V., & Thomson, J. A. (1990) *Biochemistry 29*, 2564−2572.
Pace, C. N., Laurents, D. V., & Erickson, R. E. (1992) *Biochemistry 31*, 2728−2734.
Pace, C. N., Shirley, B. A., McNutt, M., & Gajiwala, K. (1996) *FASEB J. 10*, 75−83.
Parry, R. M., Chandan, R. C., & Shahani, K. M. (1969) *Arch. Biochem. Biophys. 130*, 59−65.
Pinker, R. J., Lin, L., Rose, G. D., & Kallenbach, N. R. (1993) *Protein Sci. 2*, 1099−1106.
Privalov, P. L., & Khechinashvili, N. N. (1974) *J. Mol. Biol. 86*, 665−684.
Radzika, A., & Wolfenden, R. (1988) *Biochemistry 27*, 1644−1670.
Rose, G. D., Gierasch, L. M., & Smith, J. A. (1985) *Adv. Protein Chem. 37*, 1−109.
Serrano, L., Sancho, J., Hirshberg, M., & Fersht, A. R. (1992) *J. Mol. Biol. 227*, 544−559.
Shortle, D., Stites, W. E., & Meeker, A. K. (1990) *Biochemistry 29*, 8033−8041.
Smith, C. K., Withka, J. M., & Regan, L. (1994) *Biochemistry 33*, 5510−5517.
Takano, K., Ogasahara, K., Kaneda, H., Yamagata, Y., Fujii, S., Kanaya, E., Kikuchi, M., Oobatake, M., & Yutani, K. (1995) *J. Mol. Biol. 254*, 62−76.
Tamura, A., & Sturtevant, J. M. (1995) *J. Mol. Biol. 249*, 625−635.
Yu, M.-H., Weissman, J. S., & Kim, P. S. (1995) *J. Mol. Biol. 249*, 388−397.
Yutani, K., Ogasahara, K., Sugino, Y., & Matsusiro, A. (1977) *Nature 267*, 274−275.
Yutani, K., Ogasahara, K., Tsujita, T., & Sugino, Y. (1987) *Proc. Natl. Acad. Sci. U.S.A. 84*, 4441−4444.
Zimmerman, S. S., Pottel, M. S., Nemethy, G., & Scheraga, H. A. (1977) *Macromolecules 10*, 1−9.

BI9621829